

Pseudoatom molecular dynamicsC. E. Starrett,^{*} J. Daligault, and D. Saumon*Los Alamos National Laboratory, P.O. Box 1663, Los Alamos, New Mexico 87545, USA*

(Received 12 August 2014; published 20 January 2015)

An approach to simulating warm and hot dense matter that combines density-functional-theory-based calculations of the electronic structure to classical molecular dynamics simulations with pair interaction potentials is presented. The method, which we call pseudoatom molecular dynamics, can be applied to single-component or multicomponent plasmas. It gives equation of state and self-diffusion coefficients with an accuracy comparable to orbital-free molecular dynamics simulations but is computationally much more efficient.

DOI: [10.1103/PhysRevE.91.013104](https://doi.org/10.1103/PhysRevE.91.013104)

PACS number(s): 52.25.Kn, 51.20.+d, 51.30.+i, 52.65.Yy

I. INTRODUCTION

The challenge of accurately modeling dense plasmas over a wide range of conditions represents an unsolved problem lying at the heart of many important phenomena such as inertial confinement fusion [1], exoplanets, and white dwarfs [2,3]. The production of large scale and accurate tabulations of data such as equation of state and transport coefficients as a function of density and temperature is a formidable task, requiring a consistent quantum mechanical treatment of the many-electron problem together with a classical treatment of the nuclear motion. The atoms in the plasma may have bound states or be fully ionized, the electrons may be fully degenerate or approaching their classical limit. The nuclear fluid can range from weakly to strongly coupled. A consistent, reliable, and accurate treatment across all these physical regimes with an approach that remains computationally tractable remains as an open problem.

Plasmas of interest are typically one to thousands of times solid density, and have temperatures from about 1 eV (~ 10 kK) to thousands of eV. The difficulty of creating and controlling such plasmas in the laboratory explains the lack of experimental data to guide theoretical development, though ongoing campaigns at National Ignition Facility [4] and elsewhere (e.g., Ref. [5]), and recent advances in x-ray scattering techniques [6] are beginning to shed light on this problem.

From a simulations perspective, powerful and complex tools exist that can provide benchmark calculations. In the lower temperature regime (a few eV) one such tool is Kohn-Sham (KS) density functional theory molecular dynamics (DFT-MD) (e.g., [7]). Electrons are treated quantum mechanically through KS-DFT and ions are propagated with classical MD. The simulations are very computationally expensive and this cost scales poorly with temperature, limiting the method to lower temperatures. In practice KS-DFT-MD also relies on a pseudopotential approximation, which reduces the computational overhead by limiting the number of actively modeled electrons, through an ad hoc modification of the electron-nucleus interaction. Orbital-free (OF) DFT-MD¹ [8] does not suffer from the poor temperature scaling of KS-DFT-MD, and it has been applied to a wide range of plasma conditions (e.g., [9,10]). This benefit comes at the

cost of physical accuracy, though there has been significant recent progress in improving OFMD towards a KS-DFT-MD level of accuracy (e.g., [11,12]). However, OFMD remains computationally expensive, with typical simulations being limited to a few hundred particles and short times. It too relies on the pseudopotential approximation, so it is not an all-electron calculation.

Because of this high computational cost, wide ranging equation of state and transport properties tend to rely on much more approximate methods. Commonly used techniques include DFT-based average atom models [13–15], in which one attempts to solve for the properties of one atom in the plasma. While such models can capture the electronic structure associated with that atom reasonably well, a consistent treatment of ionic structure resulting in equation of state and transport properties of comparable accuracy to DFT-MD has never been successfully included, despite significant progress towards that goal [16–20]. The result is that ionic properties, including transport coefficients, are usually calculated more or less independently.

In this paper we report on a method for generating accurate and wide ranging equation of state and transport properties of dense plasmas, in a single, unified, and internally consistent model. The method, which we call pseudoatom molecular dynamics (PAMD), retains the computationally efficient average atom approach to the electronic structure of one pseudoatom, but couples this with consistent classical MD simulations for the ionic structure, using *ab initio* pair interaction potentials. The vastly reduced computational cost of such calculations relative to DFT-MD allows for much larger scale simulations. In short PAMD represents a solution to the problem of consistently including ionic structure and dynamics into the average atom methodology.

Another way to look at PAMD is that it is an approximate version of DFT-MD. The essential approximation is that the plasma can be thought of as an ensemble of pseudoatoms—this is known as the superposition approximation. Therefore, PAMD cannot, for example, accurately model molecules. However, this limitation is not important for most of the temperature-density regime discussed above. The important physics of bound and valence states, ion dynamics, as well as ion-ion, ion-electron, and electron-electron correlations are all included consistently. Finally, another important advantage of PAMD over DFT-MD simulations is that it does not rely on an ad hoc pseudopotential. Not only does this reduce computational complexity, but it removes uncertainty over

^{*}starrett@lanl.gov¹Hereafter referred to as OFMD.

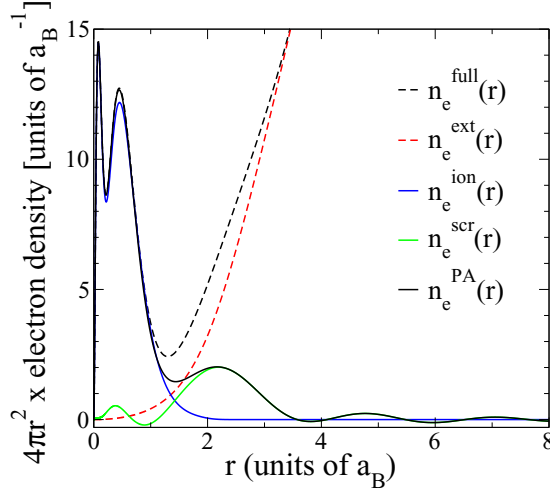


FIG. 1. (Color online) $4\pi r^2$ times electron density for aluminum at 8.1g/cm^3 and 1 eV . Shown are $n_e^{\text{full}}(r)$ (upper dashed line), $n_e^{\text{ext}}(r)$ (lower dashed line), and $n_e^{\text{PA}}(r)$, as described in the text. Also shown is the bound state (or ion) contribution [$n_e^{\text{ion}}(r)$] to $n_e^{\text{PA}}(r)$ and the valence electron contribution $n_e^{\text{scr}}(r)$ [where $n_e^{\text{PA}}(r) = n_e^{\text{ion}}(r) + n_e^{\text{scr}}(r)$]. The double peak in $n_e^{\text{ion}}(r)$ reflects the bound-state shell structure in the aluminum ion, while the oscillations in the valence contribution $n_e^{\text{scr}}(r)$ are the well-known Friedel oscillations, which are damped as temperature increases. All curves are from the Kohn-Sham version of PAMD.

possible pseudopotential artifacts. Unless otherwise stated, atomic units, in which $\hbar = m_e = k_B = e = a_B = 1$, where the symbols have their usual meaning, are used throughout.

II. THEORY

The key concept of this method is that of the pseudoatom; it is a fictitious, charge neutral object that physically represents a nucleus and its associated electron density, including bound electrons and its contribution to the valence electrons. It has been previously introduced as a statistical averaged quantity for investigation of thermodynamical properties [17,21]. Though its definition is to a certain extent arbitrary, it was recently shown [22,23] that a satisfactory definition does exist and that the pseudoatom electron density $n_e^{\text{PA}}(r)$ can be calculated efficiently in a DFT formalism, using either the orbital-free or Kohn-Sham methods. In what follows we will show results from both. The core idea for calculating $n_e^{\text{PA}}(r)$ is to first calculate an electron density $n_e^{\text{full}}(r)$ in a system with a nucleus at the origin, surrounded by a spherically averaged ionic configuration described by the ion-ion pair distribution function $g_{II}(r)$. One then calculates the electron density $n_e^{\text{ext}}(r)$ in the same system but with the central nucleus removed. $n_e^{\text{PA}}(r)$ is defined as the difference $n_e^{\text{full}}(r) - n_e^{\text{ext}}(r)$ (see Fig. 1). The physical motivation behind this is to isolate the influence of one nucleus on the electron density. Furthermore, in Ref. [23] it was demonstrated numerically that $n_e^{\text{PA}}(r)$ is insensitive to $g_{II}(r)$ for a wide range of materials, temperatures and densities and that in the linear response regime $n_e^{\text{PA}}(r)$ is independent of $g_{II}(r)$. Given this observation, one can immediately see that it should be possible to accurately

reconstruct the total electron density $n_e(r)$ of the plasma as a superposition of pseudoatom electron densities, each centered at a nuclear site

$$n_e(\mathbf{r}) = \sum_i n_e^{\text{PA}}(|\mathbf{R}_i - \mathbf{r}|), \quad (1)$$

where \mathbf{R}_i is the position vector of nucleus i , and the sum runs over all nuclear sites.

To generate the nuclear configurations $\{\mathbf{R}_i\}$ we use classical MD with pair interaction potentials in a cubic simulation cell with periodic boundary conditions, carried out in the microcanonical ensemble. An effective pair interaction potential between pseudoatoms $V_{II}(r)$ was derived in Refs. [22,23]. In Fourier space it is given by²

$$V_{II}(k) = \frac{4\pi \bar{Z}^2}{k^2} + \frac{n_e^{\text{scr}}(k)^2}{\chi_e(k)}, \quad (2)$$

where $\bar{Z} = \int d\mathbf{r} n_e^{\text{scr}}(r)$ and χ_e is the electron response function [23]. The screening density $n_e^{\text{scr}}(r)$ is the contribution to the valence electrons from the pseudoatom. It is defined by first defining the bound (or ion) states, and calculating their electron density $n_e^{\text{ion}}(r)$, so that

$$n_e^{\text{scr}}(r) = n_e^{\text{PA}}(r) - n_e^{\text{ion}}(r). \quad (3)$$

PAMD has no adjustable parameters: the inputs are the nuclear charges, atomic masses, the plasma temperature and mass density, and a choice of exchange and correlation functional.³ In Fig. 2 we show a two-dimensional (2D) slice of the electron density for a Kohn-Sham PAMD simulation with 5000 nuclei, for aluminum at 1 eV and 8.1g/cm^3 . Each circular object is a slice through a pseudoatom intersecting that plane. For those pseudoatoms whose nuclei lie closer to the plane in Fig. 2 the strong localized deformation of the electron density due to the bound electrons is visible. A simulation of this size would be very challenging for KS-DFT-MD due to computational cost, and will remain so for the foreseeable future.

In finite temperature DFT [27] the grand potential is in principle determined exactly for a given external potential once the electron density that minimizes it has been found. Thus, assuming that Eq. (1) is an accurate approximation to the equilibrium electron density for a given ionic configuration $\{\mathbf{R}_i\}$, one can determine the thermodynamic properties by using expressions based on the exact electron density. For example, in the Thomas-Fermi approximation the pressure P for a plasma of volume V with N ions and at temperature $k_B T$ ($= 1/\beta$), can be calculated using the virial formula (e.g., [28,29])

$$P V = N k_B T + \frac{2}{3} K_e^{\text{TF}} [n_e(r)] + \frac{1}{3} F^{\text{el}} [n_e(r)] + C^{\text{xc}} [n_e(r)], \quad (4)$$

where K_e^{TF} is the Thomas-Fermi approximation to the electron kinetic energy, F^{el} is the electrostatic free energy, and C^{xc} is

²Here we write the expression for plasmas with one nuclear species, the expression for mixtures is given in Ref. [24].

³For all PAMD and OFMD calculations carried out for this paper we have used the Dirac exchange functional [25] (see also Ref. [23]).

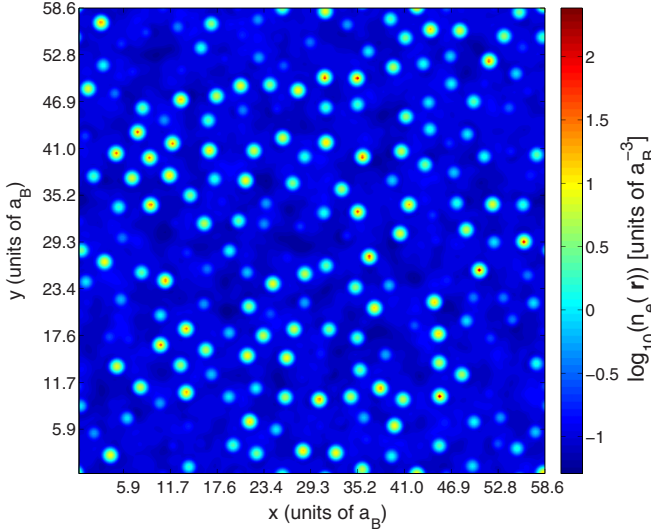


FIG. 2. (Color online) Two-dimensional (2D) slice of electron density in the Kohn-Sham version of the model for aluminum at 8.1g/cm^3 and 1 eV . The plot shows \log_{10} of the electron density. For reference \log_{10} of the average total electron density is -0.46 and \log_{10} of average screening (valence) electron density is -0.99 . The ion positions were generated in a molecular dynamics simulation with 5000 nuclei using periodic boundary conditions.

the contribution from exchange and correlations. K_e^{TF} is given by

$$K_e^{TF} = \frac{1}{\beta} \int_V d^3r c_{TF} I_{3/2}[\eta(\mathbf{r})], \quad (5)$$

where I_j is the Fermi integral of order j and $c_{TF} \equiv \sqrt{2\pi}^{-2} \beta^{-3/2}$. The electron density in this approximation is

$$n_e(\mathbf{r}) = c_{TF} I_{1/2}[\eta(\mathbf{r})]. \quad (6)$$

Thus K_e^{TF} can be calculated by inverting Eq. (6) for $\eta(\mathbf{r})$ and evaluating Eq. (5). C^{xc} and F^{el} are also straightforward to calculate given $n_e(\mathbf{r})$ from Eq. (1).

III. RESULTS

In Figs. 3 and 4 pressures calculated from PAMD using Eq. (4) are compared to OFMD simulations in the Thomas-Fermi approximation. In Fig. 3, for a pure aluminum plasma, agreement is excellent throughout the range of temperatures and for both densities. In Fig. 4 we compare pressures for an iron-helium mixture as a function of the fraction of iron in the plasma. Agreement is excellent for all iron fractions.

The advantage of using PAMD here is twofold: first, no pseudopotential is needed. Second, the calculation proceeds much more quickly. The calculation of the pseudoatom electron density and pair interaction potential takes a few minutes on a single processor. The cost of the classical MD simulations and calculation of the equation of state depends on the number of particles and the number of time steps. As an example, for the results presented in Fig. 3 we used 5000 particles and 40000 time steps; the simulations took

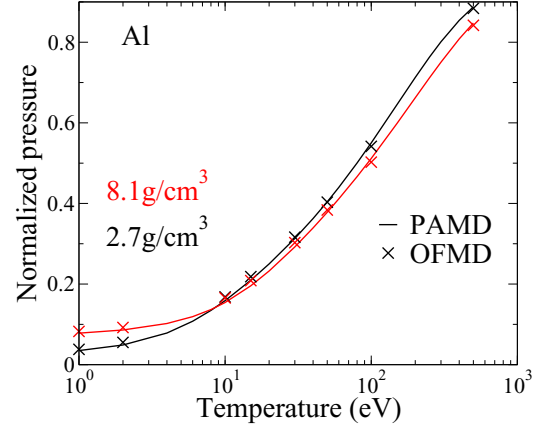


FIG. 3. (Color online) Comparison of pressure for an aluminum plasma between PAMD and OFMD in the Thomas-Fermi approximation. We show total pressure divided by the pressure of a fully ionized aluminum plasma of non-interacting classical ions and quantum electrons. Excellent agreement is found for both densities across this wide temperature range.

~ 2.5 hours per point on a compute node with two 2.3 GHz AMD Opteron 6176 processors (24 total cores) and 64 GB of random access memory. Similarly sized OFMD simulations would be extremely expensive.

Equation (4) is also valid for Kohn-Sham calculations if K_e^{TF} is replaced by the corresponding KS quantity K_e^{KS} . However, one cannot evaluate K_e^{KS} with knowledge of $n_e(\mathbf{r})$ alone as in the orbital free case. Instead K_e^{KS} depends on the Kohn-Sham wave functions (orbitals), which are not provided by PAMD. Approximate methods to determine K_e^{KS} in PAMD could be developed but we do not attempt that here.

Dynamical ion quantities such as the self-diffusion coefficient D , can be calculated with Kohn-Sham or orbital-free PAMD, since the MD simulations require only the pair interaction potential. D is calculated using the Kubo

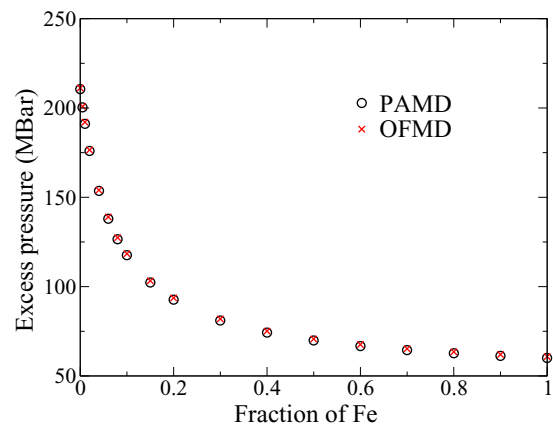


FIG. 4. (Color online) Excess pressure for a mixture of iron and helium at 10g/cm^3 and 50 eV from PAMD and OFMD [26] in the Thomas-Fermi approximation. Excess pressure is defined as the total pressure minus the ideal ion contribution (see Ref. [26]). We find excellent agreement for all mixing ratios.

TABLE I. Self-diffusion coefficients D in cm^2/s for various elements and a range of temperatures (T) and densities (ρ). The PAMD result agrees very well with the OFMD calculations, providing a very sensitive test of the PAMD pair interaction potential.

Element	ρ (g/cm^3)	T (eV)	OFMD [9,30]	OFMD (this work)	PAMD
D	1.5	2.5	0.0159	0.0146	0.0154
B	1	5	0.0162	0.0156	0.0155
B	10	5	0.00240	0.00214	0.00232
Fe	22.5	10	0.0011	0.00093	0.00105
Cu	67.4	100	0.00407	0.0039	0.00385

relation [31]

$$D = \frac{1}{3} \int_0^\infty \langle \mathbf{v}(t) \cdot \mathbf{v}(0) \rangle dt, \quad (7)$$

where $\mathbf{v}(t)$ is the velocity of a given ion in the MD simulation at time t . In Table I we compare self-diffusion coefficients for a range of materials, for various densities and temperatures, to published OFMD results [9,30], which use the Thomas-Fermi functional and a range of exchange and correlation functionals. We have also repeated these OFMD calculations using the Dirac exchange functional, and these results are also shown in Table I. The PAMD results agree very well with the OFMD calculations for all the cases. As a further test, in Fig. 5 we compare the self-diffusion coefficients for aluminum from PAMD and OFMD in the Thomas-Fermi approximation. Agreement is very good for both densities and all temperatures. These comparisons on self-diffusion coefficients represent a very sensitive test of the quality of the pair interaction potential. Such a level of agreement with an ion dynamical property is quite remarkable, given the very different approaches to the calculation of ionic forces in PAMD and OFMD. We also show for comparison in Fig. 5, the self-diffusion coefficient as calculated in PAMD using the Kohn-Sham functional. At the highest temperatures (>100 eV) there is excellent agreement between the KS and TF diffusion coefficients. We see significant deviations from the TF result below ~ 50 eV for the higher density but at the lower density agreement between the KS and TF results is reasonable above ~ 10 eV. It is expected that the Thomas-Fermi approximation will be inaccurate for the lower temperatures due to its ignorance of important quantum effects, which are captured in the Kohn-Sham calculations. The ability of Kohn-Sham based PAMD to quickly evaluate self-diffusion coefficients across temperature regimes is a significant capability, given the extreme computational cost that corresponding KS-DFT-MD simulations would entail.

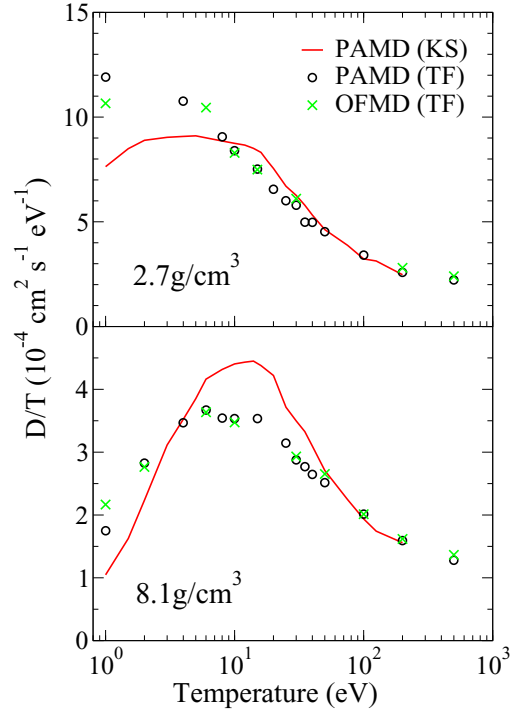


FIG. 5. (Color online) Comparison of the self-diffusion coefficient D for aluminum between PAMD and OFMD in the Thomas-Fermi approximation. Also shown is the PAMD calculation using the Kohn-Sham functional from 1–200 eV. Such a calculation would be a formidable task for the *ab initio* KS-DFT-MD method. Note that we plot D divided by temperature in eV.

IV. CONCLUSION

In conclusion we have introduced a method to simulate warm and hot dense matter that we call pseudoatom molecular dynamics. The method has proved accurate for equation of state and self-diffusion coefficients compared to orbital free molecular dynamics in the Thomas-Fermi approximation, validating the underlying physical assumption that the plasma can be considered to be an ensemble of identical pseudoatoms (at least in the TF approximation). The Kohn-Sham version of the model can be applied at high temperatures and calculations of self-diffusion coefficients for aluminum up to 200 eV have been presented. The low relative cost of PAMD permits wider ranging and larger scale investigations of the properties of warm and hot dense matter than have hitherto been possible.

ACKNOWLEDGMENTS

This work was performed under the auspices of the United States Department of Energy under Contract DE-AC52-06NA25396 and LDRD Grant No. 20130244ER.

- [1] B. A. Hammel, S. W. Haan, D. S. Clark, M. J. Edwards, S. H. Langer, M. M. Marinak, and M. V. Patel, *High Energy Density Phys.* **6**, 171 (2010).
 [2] Report of ReNew workshop, *Basic research needs for high energy density laboratory physics*, U.S. Department of Energy,

(2009), http://science.energy.gov/~media/fes/pdf/workshop-reports/hedlp_brn_workshop_report_oct_2010.pdf

- [3] G. Chabrier and E. Schatzmann, *IAU Colloquium 147, The Equation of State in Astrophysics* (Cambridge University Press, Cambridge, 1994).

- [4] A. L. Kritcher, T. Dppner, D. Swift, J. Hawreliak, G. Collins, J. Nilsen, B. Bachmann, E. Dewald, D. Strozzi, S. Felker, O. L. Landen, O. Jones, C. Thomas, J. Hammer, C. Keane, H. J. Lee, S. H. Glenzer, S. Rothman, D. Chapman, D. Kraus, P. Neumayer, and R. W. Falcone, *High Energy Density Phys.* **10**, 27 (2014).
- [5] M. D. Knudson, M. P. Desjarlais, R. W. Lemke, T. R. Mattsson, M. French, N. Nettelmann, and R. Redmer, *Phys. Rev. Lett.* **108**, 091102 (2012).
- [6] K. Falk, E. J. Gamboa, G. Kagan, D. S. Montgomery, B. Srinivasan, P. Tzeferacos, and J. F. Benage, *Phys. Rev. Lett.* **112**, 155003 (2014).
- [7] M. P. Desjarlais, J. D. Kress, and L. A. Collins, *Phys. Rev. E* **66**, 025401(R) (2002).
- [8] G. Zérah, J. Clérouin, and E. L. Pollock, *Phys. Rev. Lett.* **69**, 446 (1992).
- [9] J.-F. Danel, L. Kazandjian, and G. Zérah, *Phys. Rev. E* **85**, 066701 (2012).
- [10] P. Arnault, J. Clérouin, G. Robert, C. Ticknor, J. D. Kress, and L. A. Collins, *Phys. Rev. E* **88**, 063106 (2013).
- [11] T. Sjostrom and J. Daligault, *Phys. Rev. B* **88**, 195103 (2013).
- [12] T. Sjostrom and J. Daligault, *Phys. Rev. Lett.* **113**, 155006 (2014).
- [13] R. P. Feynman, N. Metropolis, and E. Teller, *Phys. Rev.* **75**, 1561 (1949).
- [14] D. A. Liberman, *Phys. Rev. B* **20**, 49811979.
- [15] R. Piron and T. Blenski, *Phys. Rev. E* **83**, 026403 (2011).
- [16] D. Ofer, E. Nardi, and Y. Rosenfeld, *Phys. Rev. A* **38**, 5801 (1988).
- [17] F. Perrot, *Phys. Rev. A* **42**, 4871 (1990).
- [18] B. Rozsnyai, *High Energy Dens. Phys.* **16**, 407 (2014).
- [19] B. J. B. Crowley and J. W. Harris, *J. Quant. Spectrosc. Radiat. Transfer* **71**, 257 (2001).
- [20] Yong Hou and Jianmin Yuan, *Phys. Rev. E* **79**, 016402 (2009).
- [21] J. M. Ziman, *Proc. Phys. Soc.* **91**, 701 (1967).
- [22] C. E. Starrett and D. Saumon, *Phys. Rev. E* **87**, 013104 (2013).
- [23] C. E. Starrett and D. Saumon, *High Energy Density Phys.* **10**, 35 (2014).
- [24] C. E. Starrett, D. Saumon, J. Daligault, and S. Hamel, *Phys. Rev. E* **90**, 033110 (2014).
- [25] P. A. M. Dirac, *Proc. Camb. Phil. Soc.* **26**, 376 (1930).
- [26] J.-F. Danel, L. Kazandjian, and G. Zérah, *Phys. Rev. E* **79**, 066408 (2009).
- [27] N. D. Mermin, *Phys. Rev.* **137**, A14411965.
- [28] M. T. Yin, *Phys. Rev. B* **27**, 7769 (1983).
- [29] R. M. Martin, *Electronic Structure* (Cambridge University Press, Cambridge, 2004).
- [30] F. Lambert, J. Clérouin, and S. Mazevet, *Europhys. Lett.* **75**, 681 (2006).
- [31] J.-P. Hansen and I. R. McDonald, *Theory of Simple Liquids*, 3rd ed. (Academic Press, Waltham, 2006).